JCTC Journal of Chemical Theory and Computation

Structural and Energetic Study of Cisplatin and Derivatives: Comparison of the Performance of Density Funtional Theory Implementations

Pablo D. Dans,[†] Alejandro Crespo,[‡] Darío A. Estrin,[‡] and E. Laura Coitiño*,[†]

Laboratorio de Química Teórica y Computacional, Instituto de Química Biológica, Facultad de Ciencias, Universidad de la República (UdelaR), Centro Universitario Malvín Norte, Iguá 4225, Montevideo 11400, Uruguay, and Departamento de Química Inorgánica, Analítica y Química Física/IUIMAE-CONICET, Facultad de Ciencias Exactas y Naturales, Universidad de Buenos Aires, Ciudad Universitaria, Pabellón II, Buenos Aires (C1428EHA), Argentina

Received September 18, 2007

Abstract: In this work, we compare the performance of different DFT implementations, using analytical and numerical basis sets for the expansion of the atomic wave function, in determining structural and energetic parameters of Cisplatin and some biorelevant derivatives. Characterization of the platinum-containing species was achieved at the HF, MP2, and DFT (PBE1PBE, mPW1PW91, B3LYP, B3PW91, and B3P86) levels of theory, using two relativistic effective core potentials to treat the Pt atom (LanL2DZ and SBK), together with analytical Gaussian-type basis sets as implemented in Gaussian03. These results were compared with those obtained with the SIESTA code that employs a pseudopotential derived from the Troullier−Martins procedure for the Pt atom and numerical pseudoatomic orbitals as basis set. All modeled properties were also compared with the experimental values when available or to the best theoretical calculations known to date. On the basis of the results, SIESTA is an excellent alternative to determine structure and energetics of platinum complexes derived from Cisplatin, with less computational efforts. This validates the use of the SIESTA code for this type of chemical systems and thus provides a computationally efficient quantum method (capable to linear scaling at large sizes and available in QM/MM implementations) for exploring larger and more complex chemical models which shall reproduce more faithfully the real chemistry of Cisplatin in physiological conditions.

Introduction

Cisplatin (cis-diamminedichloroplatinum(II)) is one of the most used drugs against cancer, being particularly effective in the treatment of testis, ovary, head and neck, bladder, and lung malignancies.[1] Despite the research efforts accumulated during the last 30 years addressed to elucidate the mode of action of the drug at the cellular and biochemical levels,[1,2a–e] the knowledge of the intimate chemical interactions established by the drug with relevant biomolecules (which determine cellular sensitiveness and resistance) is still at a stage far from satisfactory.[2d,e]

Reaching a deep understanding of these issues both in the case of Cisplatin and other active analogues requires not only a detailed characterization of the molecular mechanism of aquation (successive substitution of the labile ligands by water molecules, a process nowadays recognized as the activation step of these drugs in the cell)[2d] but also a complete study of the interaction and covalent binding of the drug to DNA, their pharmacological target. In the last

* To whom correspondence should be addressed. E-mail: lcoitino@luna.fcien.edu.uy. Fax: (598-2) 525 0749.

[†] Universidad de la República (UdelaR), Centro Universitario Malvín Norte.

[‡] Universidad de Buenos Aires, Ciudad Universitaria.

10.1021/ct7002385 CCC: $40.75
Published on Web 04/19/2008

two decades, theoretical and computational chemistry has started to make significant contributions on these and other related topics,[3–6] essentially by means of studies using reduced representations of the corresponding biological systems. Whereas gaining insight into the details of reactivity, interactions, and chemical processes established between platinum drugs and water/DNA requires the use of first principles quantum correlated methods—density functional theory (DFT) being the current privileged choice—size and complexity of the systems under physiological conditions turns necessary the use of hybrid quantum classical (QM/MM) descriptions to remain the study affordable. An efficient computational package available for this kind of combined quantum/classical descriptions is based upon an implementation of DFT using numerical basis sets.[7] For that reason, in this work we will validate technical choices as well as to ascertain the reliability of the outcomes of modeling regarding structure, reactivity and energetics of platinum-containing systems.

Although more than 30 articles[3–6] have appeared since the early 1980s applying quantum chemistry methods to characterize molecular properties (geometrical, electronic and vibrational, both as a goal by themselves[3a,f–i,4a,b] or aimed to develop force-field parameters[3b,c]) of Cisplatin and related compounds, participant species, thermodynamics and kinetics of aquation processes of platinum square planar complexes,[4d,5] and platination of DNA nucleobases,[4c–f,6] most of them employed implementations of the correlated theoretical level of choice—DFT within them—using different schemes of relativistic effective core potentials (ECPs) together with Gaussian-type basis sets, the use of DFT implementations with other kinds of basis sets being essentially limited to few cases addressing the most complex studies (both using plane waves[4c–f] or numerical-atomic orbitals as basis set[3f,5a,d,n,6j,k]). Only a marginal part of this work done during almost 25 years has been addressed to systematically assess the performance at the task of different quantum mechanics methods[3d,e,5b,e] (including several different DFT exchange/correlation functionals and ECPs/basis set schemes) and the relevance of including well balanced solvent/environment representations[4d–f,5b,h,j–n] in coping with some of the aforementioned issues.

A first key article pioneering in validating the use of DFT (BLYP) to describe the structure and bonding of Cisplatin, Transplatin, and their mono/diaqua-substituted derivatives was published in 1995 by Carloni et al.[4a] using plane waves for the expansion of the electronic wave function. Geometrical parameters and vibrational frequencies in fairly good agreement with the observed values were obtained, and frontier Kohn–Sham orbitals were also analyzed therein, finding for the first time a highest occupied molecular orbital—lowest unoccupied molecular orbital (HOMO–LUMO) gap consistent with experiment. Some years later, Pavankumar et al.[3d] provided a comprehensive test on the performance of HF and Möller–Plesset levels in modeling Cisplatin properties mostly using a wide range of Pople's basis sets and different ECPs schemes. More recently, whereas Wysokinski and Michalska[3e] analyzed the behavior of several pure and hybrid DFT functionals (using different ECP/basis set combinations) in predicting structural parameters, bonding and IR frequencies of Cisplatin and Carboplatin. Zhang et al. [5e] pursued a similar study focusing on the geometrical structure of Cisplatin, $PtCl_4^{2-}$, and water. Both groups agreed in selecting mPW1PW91 as the most reliable functional. However, none of these studies systematically addressed neither the performance in predicting energetics of the aquation processes (a task whose results reported by different groups have raised some controversies, their quality being sensitive to the ECP/basis set employed[5e] as well as to the description of microscopic/bulk solvent effects[5b,h,j–n]) nor that in describing bonding, thermodynamics and kinetics of the reaction between Cisplatin and DNA, even resorting to minimal models of the latter (bare nucleobases/nucleotides).

Evaluation of the existing DFT functionals and implementations, in particular those extensively used at the present for studying Cisplatin chemistry (mostly hybrid functionals), becomes necessary to calibrate and extend current knowledge to larger molecular systems and helps in the development of better methodological tools. On the other hand, the need to answer several questions in our own applied research regarding the mechanism of action of Cisplatin and related species in complex biological environments (i.e., including different double strand B-DNA sequences, Na^+ counterions and a realm of water molecules)[8] using proper structures and energetics, obtained with affordable strategies such as those present in the SIESTA (Spanish Initiative for Electronic Simulations with Thousands of Atoms) package,[7] was another practical motivation for pursuing the study presented here.

In terms of computational cost, construction of the electronic wave functions based on numerical-atomic orbitals has a great advantage over analytical localized basis sets of comparable accuracy. This approximation is used by DFT implementations in this code, providing computationally efficient quantum methods capable to linear scaling at large sizes (>100 atoms), also very efficient at intermediate molecular sizes. SIESTA uses the standard Kohn–Sham self-consistent density functional method both in the local density (LDA-LSD) and generalized gradient (GGA) approximations with norm-conserving pseudopotentials.[7] This type of quantum mechanics software can be used for the study of medium size or large systems respectively using QM (i.e., structure of the drugs and simplified representations of their chemical transformations) or QM/MM strategies (i.e., covalent interactions between water/DNA and Cisplatin under physiological conditions). To do so, validation of key issues coming from modeling against experimental data becomes mandatory, as well as comparing the performance of these implementations using numerical basis sets against other standard implementations of DFT using analytical ones, such as those currently included in GAUSSIAN[9a] or GAMESS,[9b] the main computational tools chosen in pursuing recent studies of Cisplatin and other platinated drugs interactions.[3g–i,5g–m,6q,r]

The model situations chosen in the present work to validate and compare different DFT strategies are the following: (i) Cisplatin; (ii) Cisplatin monoaqua-substituted derivative; (iii)

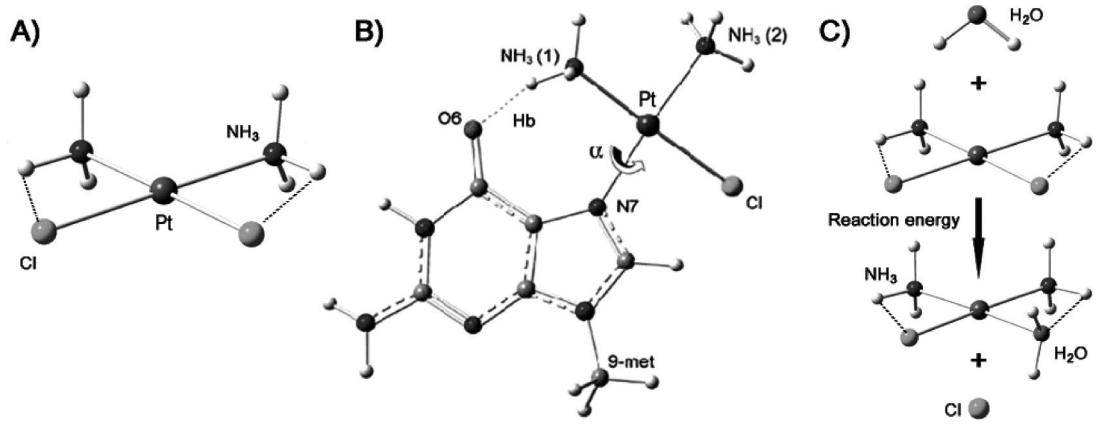

Figure 1. Schematic view of the three platinated systems studied: (A) Cisplatin; (B) Cisplatin−9metG adduct; (C) reactants and products of the first aquation process of Cisplatin. Intramolecular and intermolecular hydrogen bonds are shown with dashed lines.

Cisplatin 9-methyl-guanine adduct; and (iv) the first aquation process of Cisplatin.

Theoretical Methods

The structures of Cisplatin, 9-methyl-guanine (9metG), water, and the monoaquo complex shown in Figure 1 were fully optimized as isolated species minima, at different levels of theory using gradient techniques, without imposing any structural or symmetry constraints.

Calculations using Gaussian basis sets were performed at the HF, MP2[10] (full and frozen core), and DFT levels using the GGA functional PBE1PBE[11a] and one- to three-parameter hybrid functionals (mPW1PW91,[11b] B3LYP,[11c,d] B3PW91,[11c,e] and B3P86[11c,f]) as implemented in Gaussian03, revision B05.[9] Two ECP schemes, constituted by a pseudopotential and the concomitant double-ζ (Dζ) quality basis set, were applied for Pt as follows: (1) Stevens, Basch, and Krauss (SBK)[12a,b] ECP with CEP-31G that leads to the (7s7p5d)/[4s4p3d]-GTO valence basis set for Pt and (2) Los Alamos National Laboratory's LanL2DZ ECP developed by Hay and Wadt,[13a–d] that employs the (8s6p3d)/[5s3p2d]-GTO valence basis set for Pt. The same Pople-type basis set with polarization functions 6-31G(d)[14] is used for ligands in Cisplatin (NH_3 and Cl^-) and derivatives (H_2O and 9-methyl-guanine). The nature of the stationary points—minima—was verified at each level of theory considered here, based on the analysis of the corresponding analytical Hessian matrix.

QM computations using numerical basis sets were performed at the DFT level with SIESTA code.[7] SIESTA has shown an excellent performance for medium and large systems and has also proven to be appropriate for biomolecules and metal ions in biological systems.[15] SIESTA reads the norm-conserving pseudopotentials in semilocal form (a different radial potential $V(r)$ for each angular momentum l), generally using the Troullier−Martins parametrization.[16] Then, it transforms this semilocal form into the fully nonlocal form proposed by Kleinman and Bylander (KB).[7] The use of standard norm-conserving pseudopotentials[16] avoids the computation of core electrons, smoothing at the same time the valence charge density. Pt is treated as an 18-electron system, namely with both $n = 5$ and $n = 6$ considered as valence electron shells (Table 1 reports the reference valence configurations, cutoff radius, and total number of KB projectors used for each atom). SIESTA uses basis set functions that consist of localized (numerical) pseudoatomic orbitals (PAO), which are projected on a real space grid to compute the Hartree potential and exchange-correlation potential's matrix elements. Dζ plus polarization quality basis sets were employed for all atoms, with a PAO energy shift of 20 meV and a grid cutoff of 200 Ry.[8] To improve the thermodynamic characterization of species participating in Cisplatin aquation process, single-point calculations over the structure of the isolated species minima were carried out with a PAO energy shift of 0.5 meV and a grid cutoff of 300 Ry. Calculations were performed using the Perdew, Burke, and Ernzerhof GGA functional[10] (PBE_{SIESTA}), which coincides with the PBE1PBE functional implemented in Gaussian03 (G03).

The energy of reaction has been calculated as the subtraction between the sum of the products and the sum of the

Table 1. Reference Valence Configurations, Cutoff Radius, and Total Number of KB Projectors Used in the Troullier−Martins Procedure to Obtain the Pseudopotentials for Each Atom

atom	valence configuration	cutoff radius	no. of KB projectors
H	1s(1.00)	1.25	9
	2p(0.00)		
	3d(0.00)		
C	2s(2.00)	1.25	16
	2p(2.00)		
	3d(0.00)		
	4f(0.00)		
N	2s(2.00)	1.20	16
	2p(3.00)		
	3d(0.00)		
	4f(0.00)		
O	2s(2.00)	1.13	16
	2p(4.00)		
	3d(0.00)		
	4f(0.00)		
Cl	3s(2.00)	1.50	16
	3p(5.00)		
	3d(0.00)		
	4f(0.00)		
Pt	6s(1.00)	2.47	16
	6p(0.00)	2.87	
	5d(9.00)	1.98	
	5f(0.00)	2.30	

Table 2. Calculated Cisplatin Bond Lengths (Å) and Angles (deg) at Several Levels of Theory, OMPBDs, and OMPGDs with Respect to Experimental Values and Best Available Theoretical Data

	Pt−Cl	Pt−N	N−Pt−N	N−Pt−Cl	Cl−Pt−Cl	OMPBD	OMPGD
Pseudopotential and Basis Set Used for Pt: LANL2/LANL2DZ							
PBE1PBE	2.322 (−0.008)	2.086 (0.076)	98.2 (11.2)	83.3 (−7.0)	95.1 (3.2)[a]	2.1 [2.2][e]	5.6 [4.2]
mPW1PW91	2.324 (−0.006)	2.089 (0.079)	98.1 (11.1)	83.4 (−6.9)	95.1 (3.2)	2.1 [2.2]	5.6 [4.2]
B3LYP	2.349 (0.019)	2.110 (0.100)	98.2 (11.2)	83.3 (−7.0)	95.3 (3.4)	2.9 [2.2]	6.0 [4.3]
B3PW91	2.330 (0.000)	2.090 (0.080)	98.3 (11.3)	83.3 (−7.0)	95.1 (3.2)	2.0 [2.1]	5.6 [4.2]
B3P86	2.325 (−0.005)	2.090 (0.080)	98.4 (11.4)	83.2 (−7.1)	95.2 (3.3)	2.1 [2.2]	5.8 [4.3]
mp2(full)	2.345 (0.015)	2.093 (0.083)	97.2 (10.2)	83.8 (−6.5)	95.1 (3.2)	2.4 [1.9]	5.4 [3.8]
MP2(FC)[b]	2.347 (0.017)	2.083 (0.073)	97.4 (10.4)	83.9 (−6.4)	94.8 (2.9)	2.2 [1.6]	5.3 [3.6]
MP3(FC)[b]	2.358 (0.028)	2.098 (0.088)	96.9 (9.9)	83.9 (−6.4)	95.3 (3.4)	2.8 [1.7]	5.5 [3.7]
MP4(FC)[b]	2.358 (0.028)	2.095 (0.085)	97.1 (10.1)	84.0 (−6.3)	95.0 (3.1)	2.7 [1.6]	5.5 [3.6]
HF	2.363 (0.033)	2.124 (0.114)	95.3 (8.3)	84.5 (−5.8)	95.7 (3.8)	3.5 [2.4]	5.4 [3.5]
Pseudopotential and Basis Set Used for Pt: SBK/CEP-31G							
PBE1PBE	2.308 (−0.022)	2.093 (0.083)	98.0 (11.0)	83.5 (−6.8)	95.0 (3.1)	2.5 [2.7]	5.7 [4.3]
mPW1PW91	2.310 (−0.020)	2.095 (0.085)	98.0 (11.0)	83.5 (−6.8)	95.0 (3.1)	2.5 [2.7]	5.7 [4.3]
B3LYP	2.337 (0.007)	2.123 (0.113)	98.1 (11.1)	83.4 (−6.9)	95.2 (3.3)	3.0 [2.8]	6.0 [4.5]
B3PW91	2.316 (−0.014)	2.101 (0.091)	98.1 (11.1)	83.4 (−6.9)	95.0 (3.1)	2.6 [2.7]	5.8 [4.4]
B3P86	2.312 (−0.018)	2.095 (0.085)	98.3 (11.3)	83.3 (−7.0)	95.1 (3.2)	2.5 [2.6]	5.8 [4.4]
mp2(full)	2.307 (−0.023)	2.098 (0.088)	96.8 (9.8)	84.2 (−6.1)	94.7 (2.8)	2.7 [2.8]	5.3 [3.9]
MP2(FC)[b]	2.312 (−0.018)	2.090 (0.080)	97.1 (10.1)	84.2 (−6.1)	94.6 (2.7)	2.4 [2.5]	5.2 [3.8]
MP3(FC)[b]	2.327 (−0.003)	2.106 (0.096)	96.2 (9.2)	84.3 (−6.0)	95.2 (3.3)	2.5 [2.6]	5.1 [3.7]
MP4(FC)[b]	2.326 (−0.004)	2.105 (0.095)	96.7 (9.7)	84.2 (−6.1)	94.8 (2.9)	2.4 [2.6]	5.2 [3.8]
HF[b]	2.348 (0.018)	2.140 (0.130)	95.0 (8.0)	84.7 (−5.6)	95.7 (3.8)	3.6 [3.0]	5.4 [3.6]
Pseudopotential and Basis Set Used for Pt: Troullier−Martins/Dζ							
PBE_{SIESTA}	2.331 (0.001)	2.096 (0.086)	100.3 (13.3)	81.6 (−8.7)	96.5 (4.6)	2.2 [2.2]	6.8 [5.4]
Experimental Values (Mean and Range)[c]							
exp	2.330	2.010	87.0	90.3	91.9	0.0	0.0
exp	2.328–2.333	1.950–2.050	85.5–88.5	88.5–92.0	91.3–92.2		
Car–Parrinello Molecular Dynamics at Room Temperature[d]							
BLYP	2.36	2.03	89	88	94	[0.0]	[0.0]

[a] Values in parentheses correspond to the difference between the calculated and the mean experimental value (Δ_{c-o}) for each structural parameter. [b] Taken from ref 3d. [c] Taken from ref 17. [d] Calculated average values taken from ref 4d. [e] Values in square brackets correspond to OMPBD and OMPGD calculated with respect to the CPMD-BLYP simulation.

isolated reactants. The convenience of reporting the reaction energy considering the first aquation process as a bimolecular reaction is discussed elsewhere.[5m] In our work, BSSE was not considered.

Results and Discussion

Tables 2−6 collect representative structural parameters for Cisplatin, its monoaqua-substituted derivative, and the Cisplatin−9metG adduct as determined with each theoretical level using different combinations of functionals and ECP/basis sets (LANL2DZ, SBK and Troullier−Martins schemes). Since the aim of this work is comparing DFT implementations using analytical and numerical basis sets as respectively present in G03 and SIESTA, taking as reference the available experimental structural data,[17–19] differences between predicted and observed values (labeled as Δ_{c-o}) have been calculated and reported for all bonds and angles involving heavy-atoms. In addition, the overall mean percentage of all bond differences (OMPBD) and the overall mean percentage of all structural parameters differences (OMPGD) were calculated using Δ_{c-o} as follows:

$$\mathrm{OMPBD} = \left[\sum_{i=\mathrm{bond}}^{n} \frac{|\Delta_{c-o}|_i \times 100}{(\mathrm{BD}_{obsvd})_i}\right]\frac{1}{n} \quad (1)$$

$$\mathrm{OMPGD} = \left[\sum_{i=\mathrm{bond}}^{n} \frac{|\Delta_{c-o}|_i \times 100}{(\mathrm{BD}_{obsvd})_i} + \sum_{j=\mathrm{angle}}^{m} \frac{|\Delta_{c-o}|_j \times 100}{(\mathrm{BA}_{obsvd})_j}\right]\left(\frac{1}{n+m}\right) \quad (2)$$

BD_{obsvd} and BA_{obsvd} being respectively the observed experimental values of each of the n bond distances taken into account and each of the m bond angles considered in calculating OMPGD.

To test the performance of numerical basis set and the Troullier−Martins pseudopotential scheme against energetic parameters, reaction energy for the first aquation process of Cisplatin was calculated from the isolated species energetics and reported in Table 7. Since there is no experimental data for this reaction in gas phase, our calculations are compared to other theoretical determinations.[5b,c]

Geometry of Cisplatin. The first aspect to be taken into account is that experimental data of reference for Cisplatin come from X-ray diffraction studies in the solid state obtained by Milburn et al.[17] Due to packing interactions, distortions on the structural parameter from the gas phase are likely to be present in the solid state, hence no perfect agreement with X-ray crystallographic results are expected, even for the best theoretical method employed to determine the structure of isolated Cisplatin. Actually, the intermolecular interaction between two adjacent Cisplatin molecules present in the crystal indicated the formation of two hydrogen bonds from each nitrogen of one Cisplatin molecule, both bonds being to the same chloride atom in the next molecule along the *c*-axis of the unit cell (donor–acceptor H bond distance of 3.3 Å).[17] This H bond interaction leaves both hydrogen atoms lying in the plane of the molecule in the N−Pt−N quadrant and produces a loss of symmetry given a quasi C_{2v} conformation different than that calculated as an isolated species minimum. As a consequence, the two

Table 3. Calculated Cisplatin Monoaquo Bond Lengths (Å) and Angles (deg) at Several Levels of Theory, OMPBDs, and OMPGDs with Respect to Best Available Theoretical Data

	Pt−Cl	Pt−N[a]	Pt−O	N−Pt−N	N−Pt−Cl	N−Pt−O	O−Pt−Cl	OMPBD	OMPGD
Pseudopotential and Basis Set Used for Pt: LANL2/LANL2DZ									
PBE1PBE	2.30 (−0.03)	2.03 (0.00)	2.10 (0.00)	97 (6)	87 (−1)	87 (−7)	89 (3)[b]	0.4	2.9
mPW1PW91	2.30 (−0.03)	2.03 (0.00)	2.11 (0.01)	97 (6)	87 (−1)	87 (−7)	89 (3)	0.6	2.9
B3LYP	2.33 (0.00)	2.05 (0.02)	2.13 (0.03)	97 (6)	87 (−1)	87 (−7)	89 (3)	0.8	3.0
B3PW91	2.31 (−0.02)	2.03 (0.00)	2.11 (0.01)	97 (6)	88 (0)	87 (−7)	89 (3)	0.4	2.7
B3P86	2.30 (−0.03)	2.03 (0.00)	2.10 (0.00)	97 (6)	87 (−1)	87 (−7)	89 (3)	0.4	2.9
mp2(full)	2.32 (−0.01)	2.04 (0.01)	2.11 (0.01)	96 (5)	88 (0)	87 (−7)	89 (3)	0.5	2.5
MP2(FC)	2.32 (−0.01)	2.04 (0.01)	2.11 (0.01)	96 (5)	88 (0)	87 (−7)	89 (3)	0.5	2.5
HF	2.33 (0.00)	2.07 (0.04)	2.12 (0.02)	95 (4)	88 (0)	88 (−6)	89 (3)	1.0	2.5
Pseudopotential and Basis Set Used for Pt: SBK/CEP-31G									
PBE1PBE	2.28 (−0.05)	2.03 (0.00)	2.10 (0.00)	96 (5)	87 (−1)	87 (−7)	89 (3)	0.7	2.8
mPW1PW91	2.29 (−0.04)	2.04 (0.01)	2.10 (0.00)	96 (5)	87 (−1)	87 (−7)	89 (3)	0.7	2.8
B3LYP	2.31 (−0.02)	2.06 (0.03)	2.13 (0.03)	96 (5)	87 (−1)	87 (−7)	89 (3)	1.3	3.0
B3PW91	2.29 (−0.04)	2.04 (0.01)	2.11 (0.01)	96 (5)	87 (−1)	87 (−7)	89 (3)	0.9	2.9
B3P86	2.29 (−0.04)	2.04 (0.01)	2.10 (0.00)	97 (6)	87 (−1)	87 (−7)	89 (3)	0.7	3.0
mp2(full)	2.29 (−0.04)	2.04 (0.01)	2.10 (0.00)	96 (5)	88 (0)	87 (−7)	90 (4)	0.7	2.8
MP2(FC)	2.29 (−0.04)	2.04 (0.01)	2.10 (0.00)	96 (5)	88 (0)	87 (−7)	90 (4)	0.7	2.8
HF	2.32 (−0.01)	2.08 (0.05)	2.13 (0.03)	95 (4)	89 (1)	88 (−6)	89 (3)	1.4	2.8
Pseudopotential and Basis Set Used for Pt: Troullier−Martins/Dζ									
PBE_{SIESTA}	2.31 (−0.02)	2.03 (0.00)	2.12 (0.02)	97 (6)	86 (−2)	88 (−6)	89 (3)	0.6	2.9
Car–Parrinello Molecular Dynamics at Room Temperature[c]									
BLYP	2.33	2.03	2.10	91	88	94	86	0.0	0.0

[a] Amino group trans to water. [b] Values in parentheses correspond to the difference calculated respect to the corresponding structural parameter extracted form the best theoretical calculation known (Δ_{c-o}). [c] Calculated average values taken from ref 4d.

N−H···Cl intramolecular hydrogen bonds that appear in the gas phase (see dashed lines in Figure 1A) are substituted by two intermolecular hydrogen bonds in the crystal structure forcing the closure of the N−Pt−N angle.

For completeness and uniformity with the structural analysis of the monoaquo complex (see Table 3 and the corresponding discussion), our results for Cisplatin are also compared with the DFT Car–Parrinello molecular dynamics (CPMD-BLYP) simulation at room temperature, using periodic boundary conditions and 35 explicit water molecules to include solvent effects.[4d] The corresponding OMPBDs and OMPGDs values are reported in square brackets in Table 2.

Comparative analysis of the calculated Pt−Cl bond lengths in Cisplatin collected in Table 2 shows that whereas LanL2DZ ECP calculations essentially tend to overestimate this parameter with respect to the corresponding mean experimental values—coming from different Cisplatin molecules present in the triclinic X-ray unit cell[17]—using SBK means to underestimate it. Concerning DFT functionals and basis sets, the best results are obtained with PBE as implemented in SIESTA, as well as with the hybrid functional B3PW91 using LanL2DZ ECP for Pt. Regarding the calculated Pt−N bonds, all the methods exhibit the same trend, overestimating these distances, being the best results obtained at the MP2(FC)/LanL2DZ level, followed by both PBE1PBE/LanL2DZ and mPW1PW91/LanL2DZ, which are slightly more accurate than PBE_{SIESTA}, but still showing a very good performance comparable to that achieved at the MP4(FC) level using LanL2DZ ECP. Thus, in general terms, the LanL2DZ pseudopotential produces better results than SBK in predicting bond lengths, as reflected by the corresponding OMPBD values collected in Table 1 (B3PW91 = 2.0, PBE1PBE = 2.1, mPW1PW91 = 2.1, B3P86 = 2.1, and MP2(FC) = 2.2). In comparing results obtained with LanL2DZ and GTOs in G03 with those obtained using a numerical basis set in SIESTA, it is shown that PBE_{SIESTA} achieves a performance similar to MP2(FC) and with the DFT calculations already mentioned, but with a significantly lower computational effort. It is worthy to notice that the largest OMPBDs are obtained at the HF level indicating the importance of the inclusion of a dynamic electron correlation in the calculation of bond lengths, a fact previously reported for the Pt−Cl bond.[3d]

Considering now N−Pt−N and Cl−Pt−Cl bond angles, it can be seen that compared with experiment they are systematically overestimated—leading thus to underestimation of the N−Pt−Cl angle—by all methods disregarding any variation on the corresponding ECPs and basis set. None of the calculated bond angles fell within the experimental range. OMPGD and OMPBD values reported in Table 2 clearly show that the general performance is lower in quality when modeling angles respect to prediction of bond distances, a fact already noticed in every methodological comparison previously reported.[3d,e,5e] The Cl−Pt−Cl angle is somehow better modeled than N−Pt−N, with deviations from experiment ranging from 2.7° to 4.6°. SBK ECP gives a global better performance than LanL2DZ. In all the cases, the lack of general agreement between the observed angles and the calculated ones in gas phase are due to the already mentioned effects of packing a problem that is attenuated when comparing the data to the best available calculated structures in aqueous solution. Thus, OMPGD is only a qualitative tool at the moment of determining the global structure obtained with the different methods showing in all the cases a difference ranging from 5 to 7% (or 3.5–5.4%, depending on the nature of the data considered as a reference).

OMPBDs and OMPGDs calculated with respect to CPMD-BLYP data are close (and slightly smaller, in general terms, see Table 2) to those obtained taking X-ray crystallographic results as reference, reflecting the proximity of the structural

parameters obtained by optimization of the isolated species at 0° K to the data coming from the average over aqueous solution dynamics performed at room temperature. The principal trends already discussed are sustained in considering these values. Nevertheless, two points emerge from the analysis: (a) Möller–Plesset levels of theory become the best in predicting bond lengths for solution structures; (b) the best OMPGDs are now obtained at the HF level, probably by compensation of errors leading to a better characterization of the angles between NH_3 groups.

Geometry of Cisplatin Monoaqua-Substituted Derivative. As far as we know, there is no experimental characterization of the molecular structure of the monoaquo complex derivated from Cisplatin. The cationic complex $[Pt(H_2O)_4]^{2+}$ is the most related chemical species for which structural data obtained from EXAFS are available.[5a] The mean Pt−O bond distance reported for the tetra-aquo compound in C_{2v} conformation is 2.01 Å,[19] a value that can be thought as a semiquantitative reference for the Pt−O bond in the monoaquo species. To achieve the comparison of all bond lengths and angles that involve the heavy atoms in the monoaquo complex we have taken as a reference the values from a CPMD-BLYP simulation at room temperature, using periodic boundary conditions and 35 explicit water molecules, as previously done for Cisplatin.[4d] So we are now comparing the structural parameters calculated for isolated species with the simulated ones in aqueous solution, and thus, OMPBDs and OMPGDs collected in Table 3 were calculated using the results coming from the DFT Car–Parrinello molecular dynamics as the unique reference.

All three calculated bond lengths scarcely deviate from the reference values, showing for all methods a deviation that lies in the hundredths of angstroms. Results obtained with LanL2DZ are slightly better that the corresponding SBK ECP ones. For bond length parameters, PBE_{SIESTA} still shows a very good performance, comparable to that of mPW1PW91/LanL2DZ, with an overall agreement to the reference data (OMPBD = 0.6) placed in between the lowest quality set of results (obtained using analytical GTOs and the ECP of SBK, with OMPBDs in the 0.7–1.4 range) and the best ones achieved at the DFT/LanL2DZ levels (the lowest OMPBD value of 0.4 was obtained using PBE1PBE, B3PW91, and B3P86 functionals). Again, the small ranges spanned by all methodologies indicate that bond lengths from isolated species are fairly close to those from aqueous solution simulations.

In all cases, there is a better agreement in the two calculated bond angles involving a Cl^- ion (N−Pt−Cl and O−Pt−Cl). All methods overestimate the N−Pt−N angle, whereas the N−Pt−O angle is always underestimated a few degrees. OMPGD values ranged for all DFT functionals from 2.7 to 3.0 (being the best of them B3PW91/LanL2DZ to be compared to the best performance of 2.5 obtained at the MP2/LanL2DZ level and to a PBE_{SIESTA} performance of 2.9) showing again the excellent agreement between isolated species optimization and solvated CPMD-BLYP.

Geometry of Cisplatin−9metG Adducts. Also in this case, experimental values available for comparison come from X-ray data. As shown in Figure 2, our structural data

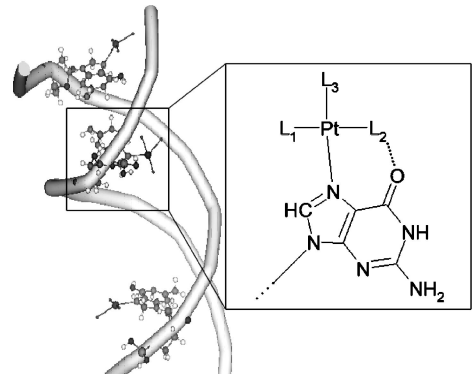

Figure 2. Schematic representation of the crystal structure (resolution: 2.6 Å) of the primary mode of binding of Cisplatin to the B-DNA dodecamer by Wing[18] et al. The PDB file (DDL017) was obtained from the Nucleic Acid Database (http://ndbserver.rutgers.edu/). The amplified sketch shows one of the formed adducts in which Cisplatin ligands are labeled as in ref 18.

obtained by optimization of isolated species under gas phase conditions are compared to data from three monofunctional adducts formed between Cisplatin (or some aquo complex derivative) and a double stranded B-DNA dodecamer of sequence d{5′-CpGpCpG*pApApTpTpCpG*pCpG-3′}{5′-CpG*pCpGpApApTpTpCpGpCpG-3′}, where the asterisk marks the sites of covalent binding (first step of platination).[18] The first inspection of the crystal structure shows the formation of three adducts in different neighbor contexts of nucleobases. Two bonds are of the type 5′-CG*C-3′, and one is of the type 5′-CG*A-3′. The binding of Cisplatin to guanine residues in different DNA sequences clearly affects, in terms of structural parameters, the formation of the Cisplatin−guanine adducts.[7] As a counterpart, the structural damage produced by platination to DNA also depends upon the specific nucleobase sequence.[7] Consistently, these aspects must be kept in mind when analyzing the experimental range and mean values reported in Table 6.

A second inspection of the X-ray structure demonstrates that the authors were not capable of determining the chemical nature of the ligands of the platinum complex (labeled L1−L3 in Figure 2).[18] It has been hypothesized that the L2 ligand could be a water molecule suggesting that the diaqua-substituted derivative was the platination agent, before crystallization was achieved.[18] Nevertheless, the knowledge of the conditions of crystallization (solution of 2-methyl-2,4-pentanediol a 4 °C)[18] and of further studies leading to determine the equilibrium relation in aqueous solution of Cisplatin, monoaquo, monohydroxo, diaquo, and dihydroxo complexes at 37 °C and different concentrations of chloride[20] allowed us to reassign the three unknown ligands as follow: L1 = Cl^- (labeled as X in Tables 4−6); L2 = N(1); and L3 = N(2).

Pt−NH_3 bond lengths calculated with all methods are in very good agreement with the experimental values taken as reference. While Pt−N(2) is always a little bit underestimated, Pt−N(1) is always overestimated by a few hundredths of angstroms. Pt−N7 bond lengths are not so well-modeled, and none of the calculated values fell within the experimental range, being for all methods shorter than expected. Calculated

Table 4. *cis*-[Pt(NH_3)$_2$Cl(9-met-guanine)]$^+$ Structure—Distances in angstroms; Angles in degress—Calculated at Several Levels of Theory Using LanL2/LanL2DZ[a]

	LANL2/LANL2DZ							
	PBE1PBE	mPW1PW91	B3LYP	B3PW91	B3P86	MP2(FC)	MP2(Full)	HF
Pt-X[b]	2.329	2.331	2.356	2.336	2.332	2.346	2.345	2.367
Pt−N(2)	2.066 (−0.055)[c]	2.069 (−0.052)	2.092 (−0.029)	2.074 (−0.047)	2.067 (−0.054)	2.085 (−0.036)	2.085 (−0.036)	2.106 (−0.015)
Pt−N(1)	2.078 (0.023)	2.081 (0.026)	2.109 (0.054)	2.088 (0.033)	2.082 (0.027)	2.082 (0.027)	2.082 (0.027)	2.130 (0.075)
Pt−N7	2.031 (−0.206)	2.033 (−0.204)	2.057 (−0.180)	2.037 (−0.200)	2.032 (−0.205)	2.024 (−0.213)	2.023 (−0.214)	2.081 (−0.156)
N(1)···O (Hb)	1.745	1.750	1.766	1.753	1.731	1.833	1.831	1.892
X[b]−Pt−N(2)	85.2 (−14.4)	85.2 (−14.4)	85.0 (−14.6)	85.2 (−14.4)	85.1 (−14.5)	85.9 (−13.7)	85.9 (−13.7)	86.2 (−13.4)
X[b]−Pt−N7	90.2 (−5.9)	90.2 (−5.9)	90.3 (−5.8)	90.2 (−5.9)	90.2 (−5.9)	89.7 (−6.4)	89.7 (−6.4)	90.3 (−5.8)
N(2)−Pt−N(1)	93.6 (11.9)	93.6 (11.9)	93.5 (11.8)	93.7 (12.0)	93.7 (12.0)	93.8 (12.1)	93.8 (12.1)	94.5 (12.8)
N(1)−Pt−N7	91.0 (10.4)	90.9 (10.3)	91.1 (10.5)	90.9 (10.3)	91.0 (10.4)	90.6 (10.0)	90.6 (10.0)	91.0 (10.4)
N(1)···O (Hb)	163	163	163	163	164	158	158	156
α	37 (11)	37 (11)	36 (10)	37 (11)	36 (10)	41 (15)	41 (15)	37 (11)
OMPBD	4.3	4.3	4.0	4.3	4.3	4.2	4.2	3.8
OMPGD	12.9	12.9	12.3	12.9	12.5	14.7	14.7	12.7

[a] Performance with respect to experimental data reported as deviations, OMPBDs and OMPGDs. [b] The nature of this ligand is not defined in the work by Wing et al.,[18] but it can be thought of as a chloride. [c] For comparison, we show in parentheses the difference between the calculated value and the mean experimental or observed value (Δ_{c-o}) taken from ref 18. See Table 6 for experimental values.

Table 5. *cis*-[Pt(NH_3)$_2$Cl(9-met-guanine)]$^+$ Structure—Distances in angstroms; Angles in deg—Calculated at Several Levels of Theory Using SBK/CEP-31G ECP[a]

	SBK/CEP-31G							
	PBE1PBE	mPW1PW91	B3LYP	B3PW91	B3P86	MP2(FC)	MP2(Full)	HF
Pt−X[b]	2.311	2.313	2.340	2.319	2.315	2.306	2.305	2.348
Pt−N(2)	2.067 (−0.054)[c]	2.070 (−0.051)	2.092 (−0.029)	2.075 (−0.046)	2.070 (−0.051)	2.074 (−0.047)	2.074 (−0.047)	2.110 (−0.011)
Pt−N(1)	2.088 (0.033)	2.090 (0.035)	2.116 (0.061)	2.096 (0.020)	2.090 (0.015)	2.089 (0.034)	2.089 (0.034)	2.128 (0.073)
Pt−N7	2.041 (−0.196)	2.043 (−0.194)	2.068 (−0.169)	2.047 (−0.141)	2.042 (−0.147)	2.029 (−0.208)	2.028 (−0.209)	2.093 (−0.144)
N(1)···O (Hb)	1.749	1.753	1.769	1.760	1.734	1.836	1.834	1.898
X[b]−Pt−N(2)	85.4 (−14.2)	85.4 (−14.2)	85.2 (−14.4)	85.3 (−14.3)	85.3 (−14.3)	86.4 (−13.2)	86.4 (−13.2)	86.3 (−13.3)
X[b]−Pt−N7	90.3 (−5.8)	90.3 (−5.8)	90.3 (−5.8)	90.3 (−5.8)	90.2 (−5.9)	89.8 (−6.3)	89.7 (−6.4)	90.3 (−5.8)
N(2)−Pt−N(1)	93.6 (11.9)	93.6 (11.9)	93.5 (11.8)	93.7 (12.0)	93.6 (11.9)	93.7 (12.0)	93.7 (12.0)	92.5 (10.8)
N(1)−Pt−N7	90.8 (10.2)	90.8 (10.2)	91.0 (10.4)	90.7 (10.1)	90.9 (10.3)	90.1 (9.5)	90.2 (9.6)	90.9 (10.3)
N(1)···O (Hb)	163	163	164	164	164	158	158	156
α	37 (11)	37 (11)	36 (10)	37 (11)	36 (10)	42 (16)	41 (15)	37 (11)
OMPBD	4.3	4.3	4.0	4.2	4.3	4.4	4.4	3.5
OMPGD	12.8	12.8	12.3	12.8	12.4	15.1	14.7	12.3

[a] Performance with respect to experimental data reported as deviations, OMPBDs and OMPGDs. [b] The nature of this ligand is not defined in the work by Wing et al.,[18] but it can be thought of as a chloride. [c] For comparison, we show in parentheses the difference between the calculated value and the mean experimental or observed value (Δ_{c-o}) taken from ref 18. See Table 6 for experimental values.

Table 6. *cis*-$[Pt(NH_3)_2Cl(9\text{-met-guanine})]^+$ Structure—Distances in angstroms; Angles in deg—Calculated with SIESTA at the PBE_{SIESTA} Level of Theory with Troullier–Martins Pseudopotentials, Deviations, OMPBDs and OMPGDs, and Reference Experimental Data

	Troullier-Martins/Dζ		
	PBE_{SIESTA}	exp (mean)	exp (range)
Pt–X[a]	2.329		
Pt–N(2)	2.066(−0.055)[b]	2.121	1.999–2.230
Pt–N(1)	2.078(0.023)	2.055	1.814–2.247
Pt–N7	2.031(−0.206)	2.237	2.164–2.315
N(1)···O(Hb)	1.745		
X[a]–Pt–N(2)	85.2(−14.4)	99.6	95.5–104.7
X[a]–Pt–N7	90.2(−5.9)	96.1	79.0–105.6
N(2)–Pt–N(1)	93.6(11.9)	81.7	78.7–85.1
N(1)–Pt–N7	91.0(10.4)	80.6	69.7–102.0
N(1)···O(Hb)	163		
α	37 (11)	26	13–44
OMPBD	4.3		
OMPGD	12.9		

[a] The nature of this ligand is not clearly defined in the work by Wing et al.,[18] but it can be thought of as a chloride. [b] For comparison purposes, difference between the calculated value and the corresponding mean experimental or observed value (Δ_{c-o}) taken from ref 18 is reported in parenthesis.

Table 7. Calculated Reaction Energy (kcal/mol) for the First Aquation Process of Cisplatin at the Different Levels of Theory over Optimized Isolated Species in the Gas Phase

	ECP/basis set employed		
level of theory	LANL2/ LANL2DZ	SBK/ CEP-31G	Troullier–Martins/Dζ
PBE1PBE/ PBE_{SIESTA}	115 (−5)	116 (−4)	142 (22)[a] 127 (7)[b]
mPW1PW91	115 (−5)	116 (−4)	
B3LYP	114 (−6)	115 (−5)	
B3PW91	115 (−5)	116 (−4)	
B3P86	119[c] (−1)	116 (−4)	
MP2(FC)	116[c] (−4)	116 (−4)	
mp2(full)	113 (−7)	115 (−5)	
HF	108 (−12)	109 (−11)	
G3-type strategy[d]	120		

[a] Results obtained from optimized structures using a PAO energy shift of 20 meV and a grid cutoff of 200 Ry. [b] Results obtained from single-point calculations over optimized structures using a PAO energy shift of 0.5 meV and a grid cutoff of 300 Ry. [c] From ref 5b. [d] For comparison purposes, differences between our calculated values and the best known theoretical value (G3-type strategy) taken from ref 5c are reported in parenthesis.

OMPBDs ranging from 3.5 to 4.4 showed good performance of all methods, HF (3.5/3.8) and B3LYP (4.0) being the most accurate ones, regardless the ECP used. PBE_{SIESTA} (OMPBD = 4.3) also gives a good overall result, comparable to the one obtained with PBE1PBE and the other hybrid functionals using analytical basis sets. MP2 (full and FC) with the ECP of SBK gave the poorest results, particularly in the description of the Pt–N7 bond.

A measure of the strength of the hydrogen bond (Hb) formed between N(1) and the O6 carbonyl group of guanine could not be obtained from the X-ray experiment since hydrogen atoms were not detected. The formation of this Hb is thought to be essential for the stabilization of the first adduct formed between Cisplatin and DNA.[6q] A recent work by van der Wijst et al., in which the performance of various density functionals in describing the hydrogen bonds in DNA base pairs was analyzed, shows that GGA functionals BP86 and PW91 gives the best results compared to X-ray values, while B3LYP tends to underestimate the hydrogen bond strength compared to experiment.[21] In our work, B3P86 gave the strongest Hb (shorter bond distance and better alignment among the three atoms involved), and if this is taken as a reference, PBE_{SIESTA} and PBE1PBE/LanL2DZ gave the following better results.

For the calculated angles, all methods give the same trends: the X–Pt–N(2) angle is systematically underestimated while the N(2)–Pt–N(1) angle is always overestimated by more than 10° and never fell within the experimental range. The X–Pt–N7 and N(1)–Pt–N7 angles are better modeled, particularly the first one, giving additional support to the reassignment of L2 as a chloride. The lowest OMPGDs in a range of 12.3–15.1 are obtained by B3LYP and B3P86 regardless of the ECP used (values of 12.3 and 12.4/12.5, respectively). For the structural characterization of the Cisplatin–9metG adduct, LanL2DZ and SBK offer the same level of accuracy. PBE_{SIESTA}, again, gives a very good result, with an accuracy comparable to PBE1PBE and the others functionals (OMPGD = 12.9). If global differences are analyzed, MP2 shows the largest deviation with respect to the experimental information. This is an outcome of a worse representation of the dihedral angle labeled α (Figure 1B), which is greatly determined by the Hb formed with the carbonyl group of guanine. A good modeling of this dihedral, that represents the angle formed between the plane of the platinum complex and the plane of the nucleobase, is crucial to estimate the stability of the adduct and the relative orientation toward the formation of the bifunctional complex (all DFT functionals and HF gave a deviation of ∼10 Å from the experimental mean value).

Energetics of the First Aquation Process of Cisplatin. A good description of the reaction energy and activation energy is decisive to understand the thermodynamic and kinetic behaviors of the reactions in which Cisplatin and its derivatives are involved. As far as we know, the best thermodynamic result obtained for the first aquation process of Cisplatin was achieved using a G3 modified strategy.[5c] The G3 modified treatment (which includes a term for describing spin–orbit coupling, uses the MWB-60 pseudopotential for the Pt and CCSD(T) instead of the original QCISD(T), replacing the G3Large basis set with the more common aug-cc-pvtz)[5c] was used as a reference to check the performance of our theoretical results when predicting the reaction energy.

As we can see in Table 7, B3P86/LanL2DZ reported by Chval and Sip[5b] gives an extraordinary good result if compared to G3. If the general accuracy of the methods used in the energetic characterization is kept in the aquation reaction of Cisplatin, we can presume that the G3 calculation does not deviate more than 1.0 kcal/mol and that the GGA and hybrid functionals accuracy rounds approximately between 3.5 and 7.5 kcal/mol apart from the probable

experimental result. This is exactly the behavior that is reproduced by the selected DFT methods that use analytical basis set functions in comparison with G3. In contrast, the results obtained from optimized species with PBE_{SIESTA} using a PAO energy shift of 20 meV and a grid cutoff of 200 Ry overestimate the calculated reaction energy by at least 22 kcal/mol leading to a worse result than HF. Nevertheless, the qualitative reaction profile is still the same in all the cases, being the first aquation process of Cisplatin in the gas phase largely endothermic.

However, if the quality of the SIESTA calculation is improved, the PBE_{SIESTA} result deviates in absolute value only 7 kcal/mol from the G3 strategy, a similar performance that MP2(full) calculations with the analytical basis functions. A comparison of PBE_{SIESTA} with PBE1PBE as implemented in G03, lead us to deduce that the Troullier−Martins pseudopotential and the numerical basis set of SIESTA also give quantitatively good results in predicting the reaction energy.

Conclusions

Our results show that SIESTA gives geometrical parameters of very good to excellent accuracy for the complexes of platinum considered herein. Particularly good results are obtained for the geometry of the Cisplatin−9metG adducts, allowing us to extend the calculations (having the performance of SIESTA in mind) to larger and more complex molecular systems. Energetic results of SIESTA show a qualitative good agreement with more standard implementations of DFT methods that use analytical basis set. However, special care should be exercised in the choice of the cutoff criteria for the pseudo-atomic orbitals to obtain a good agreement with analytical basis sets approaches.

For the description of the calculated properties, a comparison of PBE1PBE implemented in Gaussian03 and PBE_{SIESTA} allows us to state that the pseudopotential for the platinum derived with the Troullier−Martins procedure and the numerical basis set yield similar results to LanL2DZ and the Pople's basis sets employed in analytical implementations. On the basis of the quality of the results obtained for this type of systems and the computational efficiency of the numerical scheme, SIESTA results an excellent alternative as a computational tool for predicting structure and energetics of platinated systems and their transformations.

Acknowledgment. This work is part of a wider project on Cisplatin chemistry financed by CSIC-UdelaR (Uruguay) through the Research & Development (ELC, 2000–2002) and Young-Researchers (PDD, 2003–2004) programs. Sustained support from PEDECIBA (PNUD-UdelaR) during the 2000–2005 period is also gratefully acknowledged.

References

(1) Jamieson, E. R.; Lippard, S. J. Structure, Recognition, and Processing of Cisplatin-DNA Adducts. *Chem. Rev.* **1999**, *99*, 2467–2496.

(2) (a) Rosenberg, B. Platinum Complexes for the Treatment of Cancer: Why the Search Goes on. In *Cisplatin. Chemistry and Biochemistry of a Leading Anticancer Drug*; Lippert, B., Ed.; Wiley-VCH: Zürich, 1999; pp 3–27. (b) Villani, G.; Le Gac, N. T.; Hoffmann, J.-S. Replication of Platinated DNA and Its Mutagenic Consequences. In *Cisplatin: Chemistry and Biochemistry of a Leading Anticancer Drug*; Lippert, B., Ed.; Wiley-VCH: Zürich, 1999; pp 135–157. (c) Zamble, D. B.; Lippard, S. J. The Response of Cellular Proteins to Cisplatin-Damaged DNA. In *Cisplatin: Chemistry and Biochemistry of a Leading Anticancer Drug*; Lippert, B., Ed.; Wiley-VCH: Zürich, 1999; pp 73–110. (d) Fuertes, M. A.; Alonso, C.; Pérez, J. M. Biochemical modulation of Cisplatin mechanisms of action: enhancement of antitumor activity and circumvention of drug resistance. *Chem. Rev.* **2003**, *103*, 645–662. (e) Wang, D.; Lippard, S. J. Cellular Procesing of Platinum Anticancer Drugs. *Nature Rev.* **2005**, *4*, 307–320.

(3) (a) Basch, H.; Krauss, M.; Stevens, W. J.; Cohen, D. Electronic and geometric structures of $Pt(NH_3)_2^{2+}$, $Pt(NH_3)_2Cl_2$, $Pt(NH_3)_3X$, and $Pt(NH_3)_2XY$ (X, Y = H_2O, OH^-). *Inorg. Chem.* **1985**, *24*, 3313–3317. (b) Kozelka, J.; Savinelli, R.; Berthier, G.; Flament, J. P.; Lavery, R. Force field for platinum binding to adenine. *J. Comput. Chem.* **1993**, *14*, 45–53. (c) Cundari, T. R.; Fu, W.; Moody, E. W.; Slavin., L. L.; Snyder, L. A.; Sommerer, S. O.; Klinckman, T. R. Molecular Mechanics Force Field for Platinum Coordination Complexes. *J. Phys. Chem.* **1996**, *100*, 18057–18064. (d) Pavankumar, P. N. V.; Seetharamulu, S.; Yao, S.; Saxe, J. D.; Reddy, D. G.; Hausheer, F. H. Comprehensive Ab Initio Quantum Mechanical and Molecular Orbital (MO) Analysis of Cisplatin: Structure, Bonding, Charge Density, and Vibrational Frequencies. *J. Comput. Chem.* **1999**, *20*, 365–382. (e) Wysokinski, R.; Michalska, D. The Performance of Different Density Functional Methods in the Calculation of Molecular Structures and Vibrational Spectra of Platinum(II) Antitumor Drugs: Cisplatin and Carboplatin. *J. Comput. Chem.* **2001**, *22*, 901–912. (f) Hofmann, A.; Jaganyi, D.; Munro, O. Q.; Liehr, G.; van Eldik, R. Electronic Tuning of the Lability of Pt(II) Complexes through π-Acceptor Effects. Correlations between Thermodynamic, Kinetic, and Theoretical Parameters. *Inorg. Chem.* **2003**, *42*, 1688–1700. (g) Michalska, D.; Wysokinski, R. Molecular Structure and Bonding in Platinum-Picoline Anticancer Complex: Density Functional Study. *Collect. Czech. Chem. Commun.* **2004**, *69*, 63–72. (h) Wysokinski, R.; Kuduk-Jaworska, J.; Michalska, D. Electronic Structure, Raman and Infrared spectra, and vibrational assignment of Carboplatin. Density functional theory studies. *J. Mol. Struct. (Theochem)* **2006**, *758*, 169–179. (i) Wysokinski, R.; Hernik, K.; Szostak, R.; Michalska, D. Electronic structure and vibrational spectra of cis-diammine-(orotato)platinum(II), a potential Cisplatin analogue: DFT and experimental study. *Chem. Phys.* **2007**, *333*, 37–48.

(4) (a) Carloni, P.; Andreoni, W.; Hutter, J.; Curioni, A.; Giannozzi, P.; Parrinello, M. Structure and bonding in cisplatin and other Pt(II) complexes. *Chem. Phys. Lett.* **1995**, *234*, 50–56. (b) Tornaghi, E.; Andreoni, W.; Carloni, P.; Hutter, J.; Parrinello, M. Carboplatin versus cisplatin: density functional approach to their molecular properties. *Chem. Phys. Lett.* **1995**, *246*, 469–474. (c) Carloni, P.; Andreoni, W. Platinum-Modified Nucleobase Pairs in the Solid State: A Theoretical Study. *J. Phys. Chem.* **1996**, *100*, 17797–17800. (d) Carloni, P.; Sprik, M.; Andreoni, W. Key Steps of the cis-Platin-DNA Interaction: Density Functional Theory-Based Molecular Dynamics Simulations. *J. Phys. Chem. B* **2000**, *104*, 823–835. (e) Spiegel, K.; Rothlisberger, U.; Carloni, P. Cisplatin Binding to DNA Oligomers from Hybrid Car-Parrinello/Molecular Dynamics Simulations. *J. Phys. Chem. B* **2004**, *108*, 2699–2707. (f) Magistrato, A.; Ruggerone, P.; Spiegel, K.; Carloni, P.; Reedjik, J. *J. Phys. Chem. B.* **2006**, *110*, 3604–3613.

(5) (a) Deeth, R. J.; Elding, L. I. Theoretical Modeling of Water Exchange on $[Pd(H_2O)_4]^{2+}$, $[Pt(H_2O)_4]^{2+}$, and *trans*-$[PtCl_2(H_2O)_2]$. *Inorg. Chem.* **1996**, *35*, 5019–5026. (b) Chval, Z.; Sip, M. Pentacoordinated transition states of cisplatin hydrolysis-ab initio study. *J. Mol. Struct. (Theochem)* **2000**, *532*, 59–68. (c) Burda, J. V.; Zeizinger, M.; Sponer, J.; Leszczynski, J. Hydration of cis- and trans-platin: A pseudopotential treatment in the frame of a G3-type theory for platinum complexes. *J. Chem. Phys.* **2000**, *113*, 2224–2232. (d) Bergès, J.; Caillet, J.; Langlet, J.; Kozelka, J. Hydration and 'inverse hydration' of platinum(II) complexes: an analysis using the density functionals PW91 and BLYP. *Chem. Phys. Lett.* **2001**, *344*, 573–577. (e) Zhang, Y.; Guo, Z.; You, X. Hydrolysis Theory for Cisplatin and Its Analogues Based on Density Functional Studies. *J. Am. Chem. Soc.* **2001**, *123*, 9378–9387. (f) Tsipis, A. C.; Sigalas, M. P. Mechanistic aspects of the complete set of hydrolysis and anation reactions of cis- and trans-DDP related to their antitumor activity modeled by an improved ASED-MO approach. *J. Mol. Struct. (Theochem)* **2002**, *584*, 235–248. (g) Costa, L. A. S.; Rocha, W. R.; De Almeida, W. B.; Dos Santos, H. F. The hydrolysis process of the cis-dichloro(ethylendiamine)platinum(II): A theoretical study. *J. Chem. Phys.* **2003**, *118*, 10584–10592. (h) Costa, L. A. S.; Rocha, W. R.; De Almeida, W. B.; Dos Santos, H. F. The solvent effect on the aquation processes of the cis-dichloro(ethylenediammine)platinum(II) using continuum solvation models. *Chem. Phys. Lett.* **2004**, *387*, 182–187. (i) Burda, J. V.; Zeizinger, M.; Leszczynski, J. Activation barriers and rate constants for hydration of platinum and palladium square-planar complexes: An ab initio study. *J. Chem. Phys.* **2004**, *120*, 1253–1262. (j) Robertazzi, A.; Platts, J. A. Hydrogen Bonding, Solvation and Hydrolysis of Cisplatin: A Theoretical Study. *J. Comput. Chem.* **2004**, *25*, 1060–1067. (k) Raber, J.; Zhu, C.; Eriksson, L. A. Activation of anti-cancer drug Cisplatin-is the activated complex fully aquated. *Mol. Phys.* **2004**, *102*, 2537–2544. (l) Zhu, C.; Raber, J.; Eriksson, L. A. Hydrolysis Process of the Second Generation Platinum-Based Anticancer Drug cis-Amminedichlorocyclohexylamineplatinum(II). *J. Phys. Chem. B* **2005**, *109*, 12195–12205. (m) Lau, J. K.-C.; Deubel, D. V. Hydrolysis of the Anticancer Drug Cisplatin: Pitfalls in the Interpretation of Quantum Chemical Calculations. *J. Chem. Theory Comput.* **2006**, *2*, 103–106. (n) Song, T.; Hu, P. Insight into the solvent effect: A density functional theory study of Cisplatin hydrolysis. *J. Chem. Phys.* **2006**, *125*, 091101.

(6) (a) Boudreaux, E. A.; Carsey, T. P. Quasirelativistic MO Calculations on Platinum complexes (Anticancer Drugs) and their Interaction with DNA. *Int. J. Quantum Chem.* **1980**, *18*, 469–479. (b) Basch, H.; Krauss, M.; Stevens, W. J.; Cohen, D. Binding of $Pt(NH_3)_3^{2+}$ to nucleic acid bases. *Inorg. Chem.* **1986**, *25*, 684–688. (c) Zilberberg, I. L.; Avdeev, V. I.; Zhidomirov, G. M. Effect of cisplatin binding on guanine in nucleic acid: an ab initio study. *J. Mol. Struct. (Theochem)* **1997**, *418*, 73–81. (d) Pelmenschikov, A.; Zilberberg, I. L.; Leszczynski, J.; Famulari, A.; Sironi, M.; Raimondi, M. cis-$[Pt(NH_3)_2]^{2+}$ coordination to the N7 and O6 sites of a guanine-cytosine pair: disruption of the Watson-Crick H-bonding pattern. *Chem. Phys. Lett.* **1999**, *314*, 496–500. (e) Burda, J. V.; Sponer, J.; Leszczynski, J. The interactions of square platinum(II) complexes with guanine and adenine: a quantum-chemical ab initio study of metalated tautomeric forms. *J. Biol. Inorg. Chem.* **2000**, *5*, 178–188. (g) Burda, J. V.; Sponer, J.; Leszczynski, J. The influence of square planar platinum complexes on DNA base pairing. An *ab initio* DFT study. *Phys. Chem. Chem. Phys.* **2001**, *3*, 4404–4411. (h) Tsipis, A. C.; Katsoulos, G. A. Conformational preferences, rotational barriers and energetics of purine nucleobase rotation and dissociation in square planar platinum(II) antitumour complexes: Structure-activity correlation. *Phys. Chem. Chem. Phys.* **2001**, *3*, 5165–5172. (i) Deubel, D. V. On the Competition of the Purine Bases, Functionalities of Peptide Side Chains, and Protecting Agents for the Coordination Sites of Dicationic Cisplatin Derivatives. *J. Am. Chem. Soc.* **2002**, *124*, 5834–5842. (j) Baik, M.-H.; Friesner, R. A.; Lippard, S. Theoretical Study on the Stability of N-Glycosyl Bonds: Why Does N7-Platination Not Promote Depurination. *J. Am. Chem. Soc.* **2002**, *124*, 4495–4503. (k) Baik, M-H.; Friesner, R. A.; Lippard, S. J. Theoretical Study of Cisplatin Binding to Purine Bases: Why Does Cisplatin Prefer Guanine over Adenine. *J. Am. Chem. Soc.* **2003**, *125*, 14082–14092. (l) Chval, Z.; Sip, M. Transition states of cisplatin binding to guanine and adenine: ab initio reactivity study. *Collect. Czech. Chem. Commun.* **2003**, *68*, 1105–1118. (m) Burda, J. V.; Sponer, J.; Hrabakova, J.; Zeizinger, M.; Leszczynski, J. The Influence of N_7 Guanine Modifications on the Strength of Watson-Crick Base Pairing and Guanine N_1 Acidity: Comparison of Gas-Phase and Condensed-Phase Trends. *J. Phys. Chem. B* **2003**, *107*, 5349–5356. (n) Burda, J. V.; Leszczynski, J. How Strong Can the Bend Be on a DNA Helix from Cisplatin? DFT and MP2 Quantum Chemical Calculations of Cisplatin-Bridged DNA Purine Bases. *Inorg. Chem.* **2003**, *42*, 7162–7172. (o) Deubel, D. V. Factors Governing the Kinetic Competition of Nitrogen and Sulfur Ligands in Cisplatin Binding to Biological Targets. *J. Am. Chem. Soc.* **2004**, *126*, 5999–6004. (p) Jia, M.; Qu, W.; Yang, Z.; Chen, G. Theoretical study on the factors that affect the structure and stability of the adduct of a new platinum anticancer drug with a duplex DNA. *Int. J. Modern Phys. B.* **2005**, *19*, 2939–2949. (q) Raber, J.; Zhu, C.; Eriksson, L. A. Theoretical Study of Cisplatin Binding to DNA: The Importance of Initial Complex Stabilization. *J. Phys. Chem. B.* **2005**, *109*, 11006–11015. (r) Costa, L. A.; Hambley, T. W.; Rocha, W. R.; Almeida, W. B.; Dos Santos, H. F. Kinetics and structural aspects of the cisplatin interactions with guanine: A quantum mechanical description. *Int. J. Quantum Chem.* **2006**, *106*, 2129–2144.

(7) (a) Soler, J. M.; Artacho, E.; Gale, J. D.; García, A.; Junquera, J.; Ordejón, P.; Sánchez-Portal, D. The SIESTA method for ab initio order-N materials simulation. *J. Phys.: Condens. Matter* **2002**, *14*, 2745–2779. (b) Reich, S.; Thomsen, C.; Ordejón, P. Electronic band structure of isolated and bundled carbon nanotubes. *Phys. Rev. B* **2002**, *65*, 155411–155422.

(8) Dans, P. D.; Coitiño, E. L.; Crespo, A.; Estrín, D. A. Unraveling Step by Step the Molecular Choreography Ruling the Sequence-Dependent DNA Structural Changes Promoted by Cisplatin. **2008**, in preparation.

(9) (a) Frisch, M. J.; Trucks, G. W.; Schlegel, H. B.; Scuseria, G. E.; Robb, M. A.; Cheeseman, J. R.; Zakrzewski, V. G.; Montgomeri, J. A.; Stratmann, R. E.; Burant, J. C.; Dapprich, S.; Millam, J. M.; Daniels, A. D.; Kudin, K. N.; Strain, M. C.; Farkas, O.; Tomasi, J.; Barone, V.; Cossi, M.; Cammi, R.; Mennucci, B.; Pomelli, C.; Adamo, C.; Clifford, S.; Ochterski, J.; Petersson, G. A.; Ayala, P. Y.; Cui, Q.; Morokuma, K.; Malick, D. K.; Rabuck, A. D.; Raghavachari, K.; Foresman, J. B.; Cioslowski, J.; Ortiz, J. V.; Baboul, A. G.; Stefanov, B. B.; Liu, G.; Liashenko, A.; Piskorz, P.; Komaromi, I.; Gomperts, R.; Martin, R. L.; Fox, D. J.; Keith, T.; Al-Laham, M. A.; Peng, Y.; Nanayakkara, A.; Challacombe, M.; Gill, P. M. W.; Johnson, B.; Chen, W.; Wong, M. W.; Andres, J. L.; Gonzalez, C.; Head-Gordon, M.; Replogle, E. S.; Pople, J. A. *Gaussian 03*, revision B05; Gaussian Inc.: Pittsburgh, PA, 1998. (b) Schmidt, M. W.; Baldridge, K. K.; Boatz, J. A.; Elbert, S. T.; Gordon, M. S.; Jensen, J. H.; Koseki, S.; Matsunaga, N.; Nguyen, K. A.; Su, S. J.; Windus, T. L.; Dupuis, M.; Montgomery, J. A. General atomic and molecular

electronic structure system. *J. Comput. Chem.* **1993**, *14*, 1347–1363.

(10) Møller, C.; Plesset, M. S. Note on an Approximation Treatment for Many-Electron Systems. *Phys. Rev.* **1934**, *46*, 618–622.

(11) (a) Perdew, J. P.; Burke, K.; Ernzerhof, M. Generalized Gradient Approximation Made Simple. *Phys. Rev. Lett.* **1996**, *77*, 3865–3868. (b) Adamo, C.; Barone, V. Exchange functionals with improved long-range behavior and adiabatic connection methods without adjustable parameters: The mPW and mPW1PW models. *J. Chem. Phys.* **1998**, *108*, 664–675. (c) Becke, A. D. Density-functional thermochemistry. III. The role of exact exchange. *Chem. Phys.* **1993**, *98*, 5648–5652. (d) Lee, C.; Yang, W.; Parr, R. G. Development of the Colle-Salvetti correlation-energy formula into a functional of the electron density. *Phys. Rev. B* **1988**, *37*, 785–789. (e) Burke, K.; Perdew, J. P.; Wang, Y. In *Electronic Density Functional Theory: Recent Progress and New Directions*; Dobson, J. F., Vignale, G., Das, M. P., Eds.; Plenum: New York, 1998; pp 1–395. (f) Perdew, J. P. Density-functional approximation for the correlation energy of the inhomogeneous electron gas. *Phys. Rev. B* **1986**, *33*, 8822–8824.

(12) (a) Stevens, W.; Basch, H.; Krauss, J. Compact effective potentials and efficient shared-exponent basis sets for the first- and second-row atoms. *J. Chem. Phys.* **1984**, *81*, 6026–6033. (b) Stevens, W. J.; Krauss, M.; Basch, H.; Jasien, P. G. Relativistic compact effective potentials and efficient, shared-exponent basis sets for the third-, fourth-, and fifth-row atoms. *Can. J. Chem.* **1992**, *70*, 612–630.

(13) (a) Dunning, T. H., Jr.; Hay, P. J. Gaussian basis sets for molecular calculations. In *Modern Theoretical Chemistry*; Schaefer, H. F., III, Ed.; Plenum: New York, 1976; Vol. 3, pp 1–28. (b) Hay, P. J.; Wadt, W. R. Ab initio effective core potentials for molecular calculations. Potentials for the transition metal atoms Sc to Hg. *J. Chem. Phys.* **1985**, *82*, 270–283. (c) Wadt, W. R.; Hay, P. J. Ab initio effective core potentials for molecular calculations. Potentials for main group elements Na to Bi. *J. Chem. Phys.* **1985**, *82*, 284–298. (d) Hay, P. J.; Wadt, W. R. Ab initio effective core potentials for molecular calculations. Potentials for K to Au including the outermost core orbitals. *J. Chem. Phys.* **1985**, *82*, 299–310.

(14) Ditchfield, R.; Hehre, W. J.; Pople, J. A. Self-Consistent Molecular-Orbital Methods. IX. An Extended Gaussian-Type Basis for Molecular-Orbital Studies of Organic Molecules. *J. Chem. Phys.* **1971**, *54*, 724–728.

(15) (a) Crespo, A.; Marti, M. A.; Kalko, S. G.; Morreale, A.; Orozco, M.; Gelpi, J. L.; Luque, F. J.; Estrin, D. A. Theoretical Study of the Truncated Hemoglobin HbN: Exploring the Molecular Basis of the NO Detoxification Mechanism. *J. Am. Chem. Soc.* **2005**, *127*, 4433–4444. (b) Martí, M. A.; Scherlis, D. A.; Doctorovich, F. A.; Ordejón, P.; Estrin, D. A. Modulation of the NO trans effect in heme proteins: implications for the activation of soluble guanylate cyclase. *J. Biol. Inorg. Chem.* **2003**, *8*, 595–600. (c) Martí, M. A.; Capece, L.; Crespo, A.; Doctorovich, F.; Estrin, D. A. Nitric Oxide Interaction with Cytochrome c′ and Its Relevance to Guanylate Cyclase. Why does the Iron Histidine Bond Break. *J. Am. Chem. Soc.* **2005**, *127*, 7721–7728.

(16) Troullier, N.; Martins, J. L. Efficient pseudopotentials for plane-wave calculations. *Phys. Rev. B* **1991**, *43*, 1993–2006.

(17) Milburn, G. H. W.; Truter, M. R. The crystal structures of cis- and trans-dichlorodiammineplatinum(II). *J. Chem. Soc. A* **1966**, *1*, 1609–1616.

(18) Wing, R. M.; Pjura, P.; Drew, H. R.; Dickerson, R. E. The primary mode of binding of cisplatin to a B-DNA dodecamer: C-G-C-G-A-A-T-T-C-G-C-G. *EMBO J.* **1984**, *3*, 1201–1206.

(19) Hellquist, B.; Bengtsson, L. A.; Holmberg, B.; Hedman, B.; Persson, I.; Elding, L. I. Structures of solvated cations of Palladium(II) and Platinum(II) in dimethyl sulfoxide, acetonitrile and aqueous solution studied by exafs and laxs. *Acta Chem. Scand.* **1991**, *45*, 449–455.

(20) Berners-Price, S. J.; Appleton, T. G. The Chemistry of Cisplatin in Aqueous Solution. In *Platinum-Based Drugs in Cancer Therapy*; Farrell, N. P.; Kelland, L. R., Eds.; Humana Press Inc: Totowa, 2000; pp 3–35..

(21) van der Wijst, T.; Fonseca Guerra, C.; Swart, M.; Bickelhaupt, F. M. Performance of various density functionals for the hydrogen bonds in DNA base pairs. *Chem. Phys. Lett.* **2006**, *426*, 415–421.

CT7002385